Journal of Chromatography A 1692 (2023) 463838

Contents lists available at ScienceDirect

Journal of Chromatography A

journal homepage: www.elsevier.com/locate/chroma

Evaluation of the carotenoid and fat-soluble vitamin profile of industrial hemp inflorescence by liquid chromatography coupled to mass spectrometry and photodiode-array detection

Andrea Cerrato[a], Sara Elsa Aita[a], Giuseppe Cannazza[b,c], Anna Laura Capriotti[a,*], Chiara Cavaliere[a], Cinzia Citti[b,c], Chiara Dal Bosco[a], Alessandra Gentili[a], Carmela Maria Montone[a], Roberta Paris[d], Aldo Laganà[a]

[a] Department of Chemistry, Sapienza University of Rome, Piazzale Aldo Moro 5, 00185 Rome, Italy
[b] Department of Life Sciences, University of Modena and Reggio Emilia, Via Giuseppe Campi 287, 41125, Modena, Italy
[c] CNR NANOTEC, Campus Ecotekne, University of Salento, Via Monteroni, 73100 Lecce, Italy
[d] CREA - Research Centre for Cereal and Industrial Crops, Via di Corticella 133, Bologna, 40128, Italy

ARTICLE INFO

Article history:
Received 8 December 2022
Revised 27 January 2023
Accepted 30 January 2023
Available online 3 February 2023

Keywords:
Cannabis sativa
High-performance liquid chromatography
Micronutrients
Photodiode-array detection
Hemp flower

ABSTRACT

Industrial hemp (Cannabis sativa L.) is a plant matrix whose use is recently spreading for pharmaceutical and nutraceutical purposes. Detailed characterization of hemp composition is needed for future research that further exploits the beneficial effects of hemp compounds on human health. Among minor constituents, carotenoids and fat-soluble vitamins have largely been neglected to date despite carrying out several biological activities and regulatory functions. In the present paper, 22 target carotenoids and fat-soluble vitamins were analyzed in the inflorescences of seven Italian industrial hemp varieties cultivated outdoor. The analytes were extracted by cold saponification to avoid artifacts and analyzed by high-performance liquid chromatography coupled with Selected reaction monitoring mass spectrometry. Phytoene, phytofluene, and *all-trans*-β-carotene were the most abundant in all analyzed samples (31–55 μg g^{-1}, 11.6–29 μg g^{-1}, and 7.3–53 μg g^{-1}, respectively). Besides the target analytes, liquid chromatography coupled with photodiode-array detection allowed us to tentatively identify several other carotenoids based on their retention behavior and UV–vis spectra with the support of theoretical rules and data in the literature. To the best of our knowledge, this is the first comprehensive characterization of carotenoids and fat-soluble vitamins in industrial hemp inflorescence.

1. Introduction

Cannabis (*Cannabis sativa* L.) is one of the most versatile plant species historically used as a source of food, forage, fiber, oil, and narcotics [1]. Due to its remarkable genetic plasticity and ability to grow under different climatic conditions, *Cannabis sativa* L. has become a multipurpose plant species with various applications and highly sustainable, low-input cultivation [2,3]. The interest in this herbaceous plant has recently seen a resurgence because of its wide range of phytochemicals found in hemp inflorescences that have wide applications, especially in the food, pharmaceutical, and cosmetic industries [4].

Hemp inflorescences have extensively been studied in terms of the two major phytocannabinoids, i.e., the psychoactive compound Δ9-tetrahydrocannabinol (Δ9-THC) and the medicinally important and non-psychoactive compound cannabidiol (CBD) [5]. Additionally, in the last decade, minor phytocannabinoids [6], and other classes of plant chemicals, such as terpenes [7–9], phenolic compounds [7,10], lipids [11–13], and alkaloids [14], have also been extensively identified in *C. sativa*. These other plant chemicals can exert synergistic effects to enhance the bioactivities of phytocannabinoids, known as "the entourage effect" [15]. In the wide range of studied phytochemical compounds in industrial hemp, carotenoids and fat-soluble vitamins (FSV) have scarcely been considered, even though their presence is well-established in green plant tissues [16]. As micronutrients, vitamins do not provide significant energy or exert structural function, but rather perform highly specific activities for human health maintenance and metabolic integrity [17]. Vitamin A and provitamin A encompass a group of unsaturated or-

* Corresponding author at: Department of Chemistry, Università di Roma "La Sapienza", Piazzale Aldo Moro 5, 00185 Rome, Italy.
E-mail address: annalaura.capriotti@uniroma1.it (A.L. Capriotti).

https://doi.org/10.1016/j.chroma.2023.463838

ganic compounds that regulate several biological processes, including vision and immune competence [18]. Vitamin E has eight biologically active forms (four tocopherols and four tocotrienols) that exert antioxidant activity by transferring a hydrogen atom from aromatic hydroxyl groups to free radicals (reactive oxygen species, ROS) [19]. Vitamin K exists in two main forms, i.e., vitamin K_1 (phylloquinone) and vitamin K_2 (menaquinones), and carries out regulatory functions on numerous proteins, such as coagulation factors and osteocalcin [20]. Carotenoids are fat-soluble pigments with antioxidant properties biosynthesized *de novo* by plants, algae, fungi, and bacteria [21]. They possess a wide structural variety; about 750 carotenoids have been isolated from natural sources without counting geometrical isomers. Most dietary carotenoids are tetraterpenoids with a C40 skeleton, including carotenes (hydrocarbon carotenoids) and xanthophylls (oxygenated carotenoids). However, some species possessing a higher number of carbon atoms (C45 and C50) or a lower carbon number, among which apocarotenoids, norcarotenoids, and secocarotenoids have been reported [22]. The carbon skeleton can be arranged in acyclic (e.g., lycopene), monocyclic (e.g., γ-carotene), and bicyclic (e.g., α- and β-carotene) structures, and it can bear oxygenated functions such as hydroxy, keto, epoxy, aldehyde and carboxylic groups [16].

To date, only one study reported the total carotenoid concentrations in hemp inflorescences by spectrophotometric analysis in seven dioecious cultivars grown in Italy [23]. Other recent studies were instead concentrated on the detection of tocopherol isomers (α-, β-, γ-, and δ-tocopherol) and carotenoid compounds (lutein, zeaxanthin, and β-carotene) by a fluorescence detector [24] and the detection of α- and γ-tocopherol using high-performance liquid chromatography (HPLC) coupled with a UV–vis detector [25,26] in hemp seeds and hemp seed oil. Hence, for the first time, this work has aimed to obtain a comprehensive characterization of carotenoids and FSV from 7 industrial hemp flowers. To this end, the hemp inflorescences were saponified under mild temperature conditions and then analyzed by non-aqueous reversed phase (NARP) HPLC coupled to low-resolution tandem mass spectrometry (MS/MS) to quantify 22 target analytes; moreover, an untargeted screening of other carotenoids, without the support of authentic standards, was also carried out by HPLC-photodiode array (PDA) hyphenation. The overall analytical strategy led to defining a comprehensive profile of the occurring carotenoids and FSV in *Cannabis sativa* L.

2. Materials and methods

2.1. Chemicals and materials

Phytoene, phytofluene, 15-*cis*-β-carotene, 9-*cis*-β-carotene, and ζ-carotene were purchased from CaroteNature - GmbH (Switzerland). All other analytical standards, reagents used for sample preparation, and HPLC-grade solvents were purchased from Merck Life Science (Darmstadt, Germany). All individual standards had a purity higher than 86%. Butylated hydroxytoluene (BHT), provided by Merck Life Science, was used as an antioxidant both in standard solutions and during the several steps of the extraction procedure.

2.2. Hemp plant material

Five dioecious (Carmagnola, CS, Eletta Campana, Fibranova, Fibrante) and two monoecious (Codimono, Carmaleonte) hemp varieties with a chemical phenotype III (CBDA prevalent) [27] were cultivated in 2021 in Rovigo site (Veneto, Italy) in small, randomized plots with three replicates. Low-input cultivation was used, with the applications of no chemicals except nitrogen fertilization before sowing (40 units/ha) and water supply as needed. The plant material (comprising the upper part of the stem carrying inflorescences, flower bracts, apical leaves, and seeds) was collected at BBCH stage 87 [28], corresponding to the seed harvest time, and dried at 35 °C. Inflorescences, flower bracts, and apical leaves were then manually separated from the stem and seeds by a sieve with a mesh size of 1 mm. 20 g of material collected from each variety was used for the subsequent analysis.

2.3. Standard solutions

The stock solutions of the analytes were prepared by weighing at concentrations of 0.2 mg mL^{-1}. Retinol, tocopherols, and tocotrienols were solubilized in methanol with 0.1% BHT (*w/v*), and phylloquinone, menaquinone-4, and menaquinone-7 were solubilized in ethanol and freshly prepared monthly. All the other analyzed compounds were solubilized in chloroform with 0.1% BHT (w/v). The working solutions were prepared from the stock solutions by dilution at concentrations useful for the various phases of the experimental work. All the solutions were prepared using amber glassware and, when not in use, were stored in glass vials wrapped in aluminum foil at a temperature of −18 °C.

2.4. Extraction of carotenoids and fat-soluble vitamins from hemp inflorescences

Hemp samples were mashed, freeze-dried using a Heto PowerDry LL1500 (Thermo Fisher), finely ground in a mortar, and stored at - 20 °C. Three different extraction procedures were compared: (a) solid-liquid extraction (SLE), (b) maceration with an organic solvent, and (c) cold saponification.

2.4.1. Solid-liquid extraction

The SLE was performed following the procedure of Nimalaratne et al. [29]. Briefly, 10 mL of an extracting mixture consisting of hexane/ethyl acetate (9:1, *v/v*) with 0.1% (*w/v*) of BHT was added with 1 g of hemp sample and vortexed for 15 min. The mixture was then centrifuged at 3000 rpm at room temperature for 5 min and the extraction was repeated three times on the resulting biomass. The four supernatants were reunited and evaporated to 50 µL to remove most of the extracting solvent mixture while avoiding complete evaporation to preserve the integrity of the analytes in a water bath maintained at 30 °C under a slow flow of nitrogen. The samples were measured with a Hamilton glass syringe and diluted to a final volume of 200 µL with 2-propanol/hexane (75:25, *v/v*) solution containing 0.1% (*w/v*) of BHT.

2.4.2. Maceration with an organic solvent

Cold static maceration was performed using hexane/2-propanol (80:20, *v/v*) with 0.1% (*w/v*) of BHT. One g of hemp was macerated overnight (15 h) with 10 mL of extracting solution. The mixture was centrifuged at 3000 rpm at room temperature for 5 min and the supernatant was evaporated to 50 µL in a water bath maintained at 30 °C under a slow flow of nitrogen and diluted to a final volume of 200 µL with 2-propanol/hexane (75:25, *v/v*) solution containing 0.1% (*w/v*) of BHT.

2.4.3. Cold saponification

The cold saponification was performed following the workflow of Gentili et al. [30] with minor modifications. Briefly, 1 g of freeze-dried hemp inflorescences was transferred to a 50 mL polypropylene centrifuge tube with a screw cap. Twelve milliliters of pure ethanol containing 0.1% BHT (*w/v*) and 2 mL of 50% (*w/v*) aqueous KOH were added. After releasing the headspace with nitrogen, the tube was promptly closed and placed in a water bath maintained at 25 °C under magnetic stirring overnight (15 h). After incubation, the digested was diluted with 6 mL of water, and the analytes were extracted with 5 mL of hexane with 0.1% (*w/v*)

Table 1
APCI MS parameters optimized for SRM acquisition of the analytes selected in this study on hemp.

Analyte	Retention time (average ± SD, min)	Qualifier and quantifier SRM transitions (*m/z*)	Ion ratio (average ± SD,%)
retinol	3.3 ± 0.6	269.0/107.1 269.0/93.1	29 ± 3
δ-tocotrienol	6.5 ± 0.3	397.4/177.3 397.4/137.2	75 ± 5
β- + γ-tocotrienol	7.9 ± 0.4	411.4/191.2 411.4/151.2	65 ± 7
α-tocotrienol	8.2 ± 0.5	425.3/205.5 425.3/165.2	31 ± 5
δ-tocopherol	8.1 ± 0.4	402.4/137.0 402.4/177.2	76 ± 7
β- + γ-tocopherol	8.8 ± 0.5	416.3/191.2 416.3/151.1	20 ± 5
α-tocopherol	9.5 ± 0.4	430.2/205.1 430.2/165.1	9 ± 2
menaquinone-4	8.2 ± 0.5	445.3/227.2 445.3/187.1	25 ± 3
all-trans-lutein	9.9 ± 0.2	551.5/135.2 551.5/175.0	61 ± 4
all-trans-zeaxanthin	10.0 ± 0.3	551.6/175.0 569.4/177.2	50 ± 2
menaquinone-7	10.0 ± 0.4	649.6/227.4 649.6/187.1	4 ± 1
canthaxanthin	10.1 ± 0.5	565.7/133.2 565.5/203.3	53 ± 7
all-trans-β-cryptoxanthin	10.4 ± 0.5	553.5/135.1 553.5/119.1	56 ± 3
phylloquinone	11.1 ± 0.4	451.5/199.2 451.5/187.3	18 ± 5
phytoene	14.8 ± 0.6	545.5/69.0 545.5/81.0	74 ± 9
phytofluene	15.1 ± 0.3	543.4/69.0 543.4/81.0	80 ± 7
15-*cis*-β-carotene	17.2 ± 0.3	537.0/119.0 537.0/177.0	61 ± 4
all-trans-ζ-carotene	17.9 ± 0.5	541.7/81.0 541.7/69.0	97 ± 9
all-trans-β-carotene	18.1 ± 0.2	537.0/119.0 537.0/177.0	61 ± 5
9-*cis*-β-carotene	18.8 ± 0.4	537.0/119.0 537.0/177.0	61 ± 7

of BHT. The mixture was stirred magnetically for 5 min, then vortexed for 5 min and centrifuged at 6000 rpm for 5 min to facilitate the separation of the insoluble residue, the aqueous phase, and the organic phase. The extraction was repeated four times. The hexane extracts from each extraction were combined and washed with 6 mL of water; two washes were enough to remove the alkalis altogether. Finally, the extract was collected in a new tube and evaporated to 50 µL in a water bath maintained at 30 °C under a slow flow of nitrogen and diluted to a final volume of 200 µL with 2-propanol/hexane (75:25, *v/v*) solution containing 0.1% (*w/v*) of BHT.

2.5. High-performance liquid chromatography-tandem mass spectrometry

The analysis was performed using a Perkin Elmer 200 series binary pump equipped with an autosampler (Perkin Elmer, Norwalk, CT, USA) an Applied Biosystem API 3000 triple quadrupole mass spectrometer (Applied Biosystem Sciex, Ontario, Canada), set to acquire in Selected Reaction Monitoring (SRM) scan mode. Analytes were separated with ProntoSIL C_{30} column (4.6 mm × 250 mm, 3 µm) by Bischoff chromatography (Leonberg, Germany), protected by a C_{30} guard column (4.0 mm × 10 mm, 5 µm), in NARP conditions at a temperature of 19 °C. The mobile phases used were methanol (phase A) and a mixture of 2-propanol and hexane (50:50, *v/v*; phase B), and the gradient was as follows: 0–1 min, 0% B; 1–15 min, 0–75% B; 15–15.1 min, 75–99.5% B; and 15.1–30.1 min, 99.5% B. The mobile phase was fully introduced into the MS detector at a flow rate of 1 mL min^{-1}. Phase B was also used for flushing the autosampler injection device.

Analytes were detected in positive ion mode by placing the atmospheric pressure chemical ionization probe (APCI) in the Turbo V source and setting a needle current (NC) of 3 µA and a probe temperature of 450 °C. High purity nitrogen was used as curtain gas (2 L min^{-1}) and collision gas (4 mTorr), while air as nebulizer gas (1.5 L min^{-1}) and make-up gas (2 L min^{-1}). A polypropylene glycol solution was infused at 10 µL min^{-1} to calibrate at the unit resolution of each Q1 and Q3 quadrupole; the unit mass resolution was established and maintained in the mass resolution quadrupoles while maintaining a full width at half maximum (FWHM) of approximately 0.7 ± 0.1 Da.

For quantitative analysis of the analytes, two SRM transitions were selected, after observing their product ion scan spectra, by flow injection analysis (10 ng injected; 1 mL min^{-1} flow rate). Table 1 summarizes the most important HPLC–APCI(+)-MS/MS parameters useful for analyzing the selected target compounds. β and γ isomers of tocopherol and tocotrienol were not separated by the NARP LC separation nor distinguished by their MS behavior. The fragmentation pathways of tocopherols/tocotrienol consist in the cleavage of the alkyl chain and the obtention of product ions of the stable aromatic section of the molecule that vary for the number of methyl substituents (α vs β isomers) but not their position (β vs γ isomers) [31]. As such, the two standards injected individually furnished the same SRM transitions and non-statistically

different ion ratios, and the γ-isomers were employed for the development of the method. Therefore, the two pairs of isomers were analyzed and quantified as mixtures. The confirmation of the identified analytes was based on the criteria expressed in Commission Decision 2002/657/EC [32]; each analyte was identified based on its retention time, the two selected SRM transitions, and their relative abundance.

2.6. Method validation

The HPLC-SRM method for analyzing carotenoids and fat-soluble vitamins in hemp inflorescences was performed following the main FDA guidelines using pooled samples of all hemp analyzed. The parameters evaluated were recovery (RE), matrix effect (ME), interday and intraday precision, linear dynamic range, limits of detection (LODs), and limits of quantitation (LOQs). REs were calculated on three 1-g replicates from the pool spiked with the analytes at two different concentration levels (C_a 5 µg g^{-1} and C_b 70 µg g^{-1} for *all-trans*-β-carotene, phytoene, and phytofluene, C_a 0.25 µg g^{-1} and C_b 10 µg g^{-1} for all other analytes) according to Eqs. (1). All aliquots were extracted as described in Section 2.3, and the peak areas were compared to those of another 1-g aliquot fortified after extraction with the same standard amount (SIM). $Area_{Ca,b}$ and $Area_{SIM}$ were both subtracted by the preexisting target compound area ($Area_{C0}$).

$$RE\% = \frac{Area_{Ca,b} - Area_{C0}}{Area_{SIM} - Area_{Co}} \text{ x } 100 \quad (1)$$

MEs were calculated by comparing the $Area_{SIM}$ of each targeted compound (subtracted by the preexisting targeted compound $Area_{C0}$) and the area of the same targeted compound dissolved in the reconstitution solvent without extraction ($Area_{Rif}$). A ME value of 100% indicates no matrix effect, whereas for ME values lower and higher than 100% there are ionization suppression and enhancement, respectively.

$$ME\% = \frac{Area_{SIM} - Area_{C0}}{Area_{Rif}} \text{ x } 100 \quad (2)$$

Intraday precision was calculated as the mean recovery's relative standard deviation (RSD), whereas the interday precision was calculated as the RSD of the recoveries obtained from 5 replicates performed on 5 different days.

Calibration curves were built by analyzing seven aliquots of the hemp pool (C_0 – C_6), six of which were fortified (C_1 – C_6) before extraction with increasing concentrations of the standards (for the applied fortification levels see Table S1 in the Supplementary Material). Before constructing a calibration curve, the peak area detected in the C_0 aliquot was subtracted from the peak areas of the C_1 – C_6 calibrators. Then, the resulting peak area was plotted against the fortification level (µg g^{-1}). Since precise measurement of the signal-to-noise ratio cannot be performed for the standard addition method [33], LODs and LOQs were estimated by examining the target compound peaks in comparison with the width of the fluctuating basal noise just before and after the peak, except for the three targeted compounds that were not measured in all or some samples.

2.7. High-performance liquid chromatography-photodiode array

The experiments were conducted using a 200 series micro-HPLC (Perkin-Elmer, Norwalk, CT, USA) coupled with a 200 series diode array detector (Perkin-Elmer). The chromatographic conditions were those already described in Section 2.4. A Z-flow cell (12 µL volume; 10 mm optical path) was used with the PDA. LC-PDA chromatograms were acquired at 450 nm (λ_{max} of all trans-β-carotene, all-trans-zeaxanthin and all-trans-β-cryptoxanthin) with a bandwidth of 10 nm. The UV–Vis spectra were recorded at 200–700 nm. Totalchrom Navigator 6.3.1 and Iris (Perkin-Elmer) were used to control the instrument and data collection, respectively.

2.8. Statistical analysis

MetaboAnalyst 5.0 was employed for statistical analysis of the carotenoid and FSV datasets [34]. The data matrix was submitted as a text file that was prepared according to the specific indications that are furnished by the developers. The interquartile range (IQR) was selected for data filtering, whereas the autoscaling algorithm was selected for data scaling. For data analysis, a hierarchical clustering heatmap was chosen using the normalized datasets and the following parameters: (i) standardization: autoscale features; (ii) distance measure: Euclidean; (iii) clustering method: Ward. Moreover, an unsupervised chemometric approach based on the principal component analysis (PCA) was carried out.

3. Results and discussion

3.1. Choice of the extraction procedure

At first, three different extraction procedures, based on an SLE, maceration with an organic solvent, and a cold saponification process, were evaluated to compare recoveries and matrix effects. For this purpose, a quality control sample consisting of a pool of all the analyzed cannabis accessions was employed. The SLE was selected for being the simplest and most rapid approach for carotenoid and FSV extraction. On the other hand, maceration has widely been proposed for carotenoid and FSV extraction since it does not require heating systems, which would cause the thermal degradation of carotenoids [35].

Whereas carotenoids (e.g., β-carotene) are commonly present in their free forms in plant matrices, xanthophylls, which bear hydroxyl groups, are often found in more stable esterified forms with fatty acids such as myristic, palmitic, and stearic acid [36]. Therefore, the extraction of carotenoids and FSV have often been performed in combination with saponification processes [37]. Despite being the most common approach for the hydrolysis of neutral lipids, hot saponification could cause the isomerization of carotenoids and the degradation of vitamin K vitamers and xanthophylls [37]. Therefore, milder conditions were chosen. For the choice of extraction method, RE and ME were measured at C_a concentration levels. In HPLC–MS/MS, matrix effects are combined consequences between the influence of the matrix entering the ion source and the chemical nature of the target compound. The heterogeneous environment of inflorescence matrices results in a competition between analyte ions and other matrix components. This competition leads to an effective decrease (ion suppression) or increase (enhancement) in the ionization process, expressed as the absolute matrix effect, and shows high analyte/matrix-dependent differences.

The three tested protocols had a similar RE of about 70–100%, but the ME were closer to 100% for cold saponification compared to the other two extraction protocols (Table S2). This can be explained by considering that cold saponification effectively removes chlorophylls separating it from other liposoluble compounds [38]. The removal of neutral lipids has also a positive effect on the chromatographic separation, identification, and quantification of carotenoids and FSV.

3.2. Validation results

The validation of the cold saponification-HPLC-MS/MS method for analyzing carotenoids and FSV in hemp inflorescences was performed in accordance with the main FDA guidelines using the hemp pool sample. The proposed approach was evaluated based on

Table 2
Results of the quantitative analysis of carotenoids and fat-soluble vitamins in industrial hemp flowers from different cannabis strains (μg g^{-1}).

Compound	CS	Carmagnola	Carmaleonte	Codimono	Eletta Campana	Fibrante	Fibranova
retinol	0.15 ± 0.05	0.22 ± 0.05	0.5 ± 0.2	0.30 ± 0.09	0.23 ± 0.08	0.33 ± 0.09	0.22 ± 0.09
δ-tocotrienol	n.d.	n.d.	n.d.	n.d.	n.d.	n.d.	n.d.
β- + γ-tocotrienol	0.027 ± 0.007	0.025 ± 0.009	0.028 ± 0.008	0.037 ± 0.005	0.020 ± 0.006	0.027 ± 0.008	0.04 ± 0.02
α-tocotrienol	0.059 ± 0.005	0.07 ± 0.01	0.010 ± 0.002	0.073 ± 0.005	0.07 ± 0.02	0.12 ± 0.02	0.11 ± 0.01
δ-tocopherol	0.057 ± 0.001	n.d.	n.d.	n.d.	0.057 ± 0.007	0.05 ± 0.01	n.d.
β- + γ-tocopherol	0.61 ± 0.07	0.5 ± 0.1	0.5 ± 0.2	0.5 ± 0.3	0.7 ± 0.3	0.58 ± 0.01	0.40 ± 0.09
α-tocopherol	1.7 ± 0.3	1.3 ± 0.4	0.65 ± 0.08	1.5 ± 0.4	1.0 ± 0.7	3.0 ± 0.3	0.9 ± 0.3
menaquinone-4	0.9 ± 0.4	0.44 ± 0.08	1.0 ± 0.1	1.1 ± 0.3	0.4 ± 0.1	0.9 ± 0.2	1.1 ± 0.4
all-trans-lutein	0.3 ± 0.1	0.10 ± 0.02	0.14 ± 0.06	0.3 ± 0.2	0.11 ± 0.03	0.12 ± 0.02	0.12 ± 0.02
all-trans-zeaxanthin	6.5 ± 0.3	1.6 ± 0.1	0.4 ± 0.1	0.6 ± 0.2	1.5 ± 0.2	1.6 ± 0.1	0.12 ± 0.03
menaquinone-7	n.d.	n.d.	0.15 ± 0.09	n.d.	n.d.	n.d.	n.d.
canthaxanthin	0.05 ± 0.01	0.07 ± 0.03	0.04 ± 0.01	0.052 ± 0.007	0.05 ± 0.02	0.05 ± 0.03	0.05 ± 0.03
all-trans-β-cryptoxanthin	2.2 ± 0.2	2.4 ± 0.1	0.7 ± 0.3	2.4 ± 0.2	2.3 ± 0.3	2.5 ± 0.1	2.8 ± 0.2
phylloquinone	1.02 ± 0.06	2.0 ± 0.1	0.4 ± 0.2	0.8 ± 0.2	0.77 ± 0.06	1.7 ± 0.5	0.8 ± 0.1
phytoene	36 ± 9	36 ± 3	55 ± 8	43 ± 6	40 ± 10	31 ± 3	46 ± 9
phytofluene	13 ± 2	11.6 ± 0.3	29 ± 4	21 ± 4	14 ± 3	12 ± 2	19 ± 4
15-*cis*-β-carotene	0.76 ± 0.07	1.1 ± 0.3	0.3 ± 0.1	1.3 ± 0.3	1.3 ± 0.6	1.1 ± 0.3	1.2 ± 0.4
all-trans-ζ-carotene	0.10 ± 0.05	0.12 ± 0.02	0.24 ± 0.08	0.18 ± 0.04	0.08 ± 0.03	0.11 ± 0.03	0.14 ± 0.05
all-trans-β-carotene	33 ± 6	39 ± 6	7.3 ± 0.4	41 ± 5	44 ± 9	35 ± 3	53 ± 4
9-*cis*-β-carotene	0.6 ± 0.2	0.9 ± 0.2	0.2 ± 0.1	0.91 ± 0.09	0.9 ± 0.3	0.76 ± 0.02	1.2 ± 0.2

RE, interday and intraday precision, linear regression parameters, LODs, and LOQs. The validation results are summarized in Table S3. RE values were determined at two fortification levels (C_a and C_b) in hemp inflorescences samples, according to Eqs. (1). Since the β and γ isomers of tocopherol and tocotrienol were not separated by the chromatographic system, the two pairs were evaluated in combination. For all investigated analytes except menaquinone-4, RE values were > 70% at both C_a and C_b, which were close to the lower and upper values of the considered linear dynamic range, respectively. Among the analyzed compounds, the vitamin K vitamers (phylloquinone, menaquinone-4, and menaquinone-7) showed the lowest RE values, in agreement with previous findings following saponification [37]. The intraday and interday precision was evaluated by performing recovery experiments ($n = 5$) on the same day and five consecutive days and measuring the RSD. The intraday precision was below 10% for all analytes, whereas the interday precision was below 15% for all analytes except the vitamin K vitamers menaquinone-4 and menaquinone-7. The linear dynamic range was evaluated taking into consideration the preexisting targeted compound amounts that were estimated from the hemp pool analysis. Square linear regression coefficients (R^2) were > 0.99 for all analytes, except the vitamin E vitamers for which R^2 were between 0.95 and 0.99. Since LOD and LOQ values are matrix-dependent in LC-MS/MS, a direct comparison of our results cannot be made. However, the values are in line with or even better than previously reported results using similar approaches on other matrices [37,39,40].

3.3. Carotenoid and fat-soluble vitamin content in hemp inflorescence of different varieties

Following the validation of the LC-MS/MS method on the hemp flower pool, the individual hemp varieties were analyzed. Seven Italian hemp cultivars, i.e., Carmagnola, CS, Carmaleonte, Codimono, Eletta Campana, Fibrante, and Fibranova, were considered, and, for each cultivar, three distinct samples from different areas of the experimental field were collected. The quantitative results are summarized in Table 2 expressed as absolute concentrations and in Table S4 as percentages. To the best of our knowledge, there have been no previous papers that focused specifically on the characterization of carotenoids and FSV in hemp inflorescence. However, Spano et al. [23]. have previously estimated the total carotenoid content of seven hemp cultivars via spectrophotometric analysis, resulting in 106–317 μg g^{-1} depending on each accession and harvesting time. On average, our LC-MS/MS results furnished 104.5 μg g^{-1}, ranging from 90.9 μg g^{-1} for Fibrante samples to 127.2 μg g^{-1} for Fibranova samples. It is important to highlight that, despite being somehow similar, a direct comparison of our results to those of Spano could be misleading. First, our analysis considered the contribution of only 22 analytes, whereas, as shown later, there are possibly several other carotenoids in hemp inflorescence. Moreover, the spectrophotometric analysis could underestimate the content of UV-absorbing carotenoids (e.g., phytoene) and be affected by non-carotenoid interference.

Among the 22 analytes considered, 19 were found in all industrial hemp varieties, δ-tocopherol was found in CS, Eletta Campana, and Fibrante samples, menaquinone-7 was detected in the sole Carmaleonte sample, and δ-tocotrienol was detected in none. Phytoene, β-carotene, and phytofluene were the three most abundant carotenoids in all analyzed samples (Fig. 1), ranging between 84.5% and 94.6% (90% on average) of the total carotenoid content.

Phytoene is a UV-absorbing carotenoid precursor that is synthesized in plants by the phytoene synthase enzyme by coupling two geranylgeranyl pyrophosphate units and undergoes a series of desaturation and cyclization reactions that produce all other carotenoids, starting with phytofluene [41]. Phytoene and phytofluene have gathered attention for their skin protection activity since they absorb in the UVB-UVC and UVA regions, respectively [42]. On the other hand, β-carotene is a deeply colored carotenoid that is converted to vitamin A (retinol) by the β-carotene 15,15′-dioxygenase [43]. As such, vitamin A (retinol) and provitamin A (β-carotene and β-cryptoxanthin) vitamers represented on average 36.4% of the total carotenoid content, whereas vitamin E vitamers (α-, β-, γ-, δ-tocopherols and α-, β-, γ-, δ-tocotrienols) and vitamin K vitamers (menaquinone-4, menaquinone-7, and phylloquinone) represented the 2.1% and 1.9%, respectively. Among the vitamin E vitamers, α-tocopherol was the most abundant with more than two-thirds of the total vitamin E content, followed by β- + γ-tocopherols. These results are in striking contrast with previous findings on hempseeds and hempseed oil that showed γ-tocopherol as the main vitamer [24,44]. In general, the carotenoid profile of hemp inflorescence seems rather different compared to that of hempseeds. Irakli et al. [24], in fact, demonstrated that tocopherols are over ten times more abundant than β-carotene in hempseeds, whereas our results show the opposite trend. This result also suggests a different regulation of the carotenoid biosynthesis among plant organs even if no information is available yet on this pathway in Cannabis.

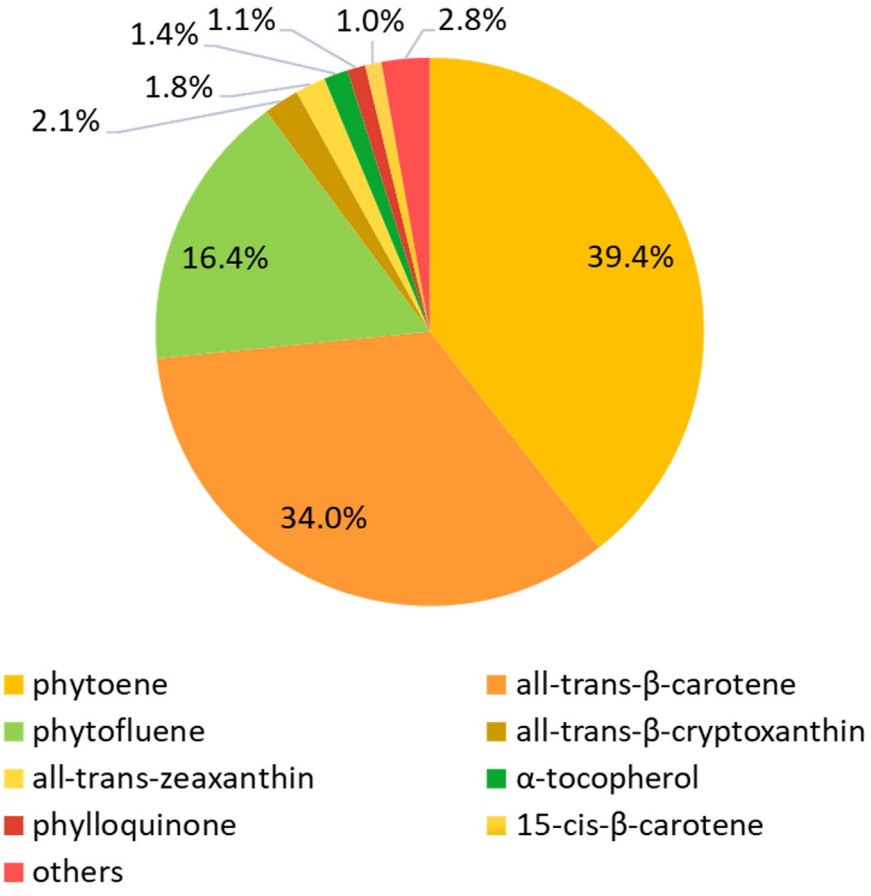

Fig. 1. Pie chart showing the average content of the analyzed carotenoids in industrial hemp inflorescence.

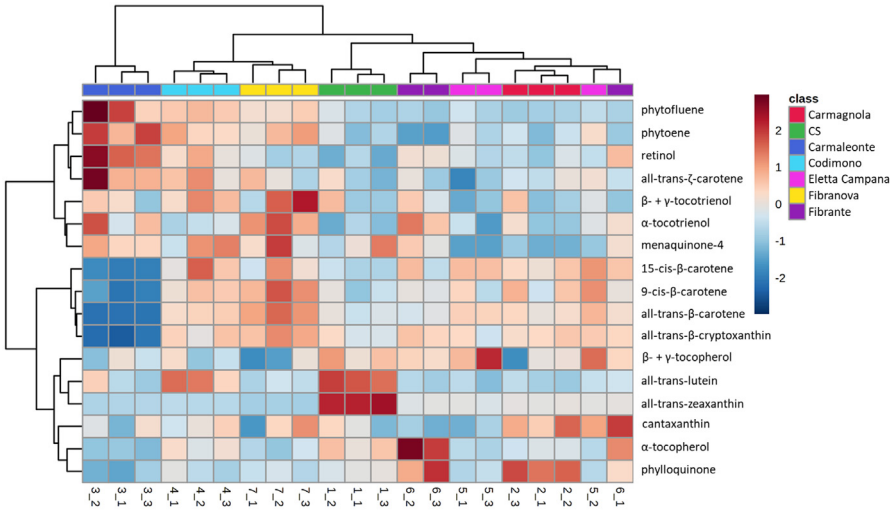

Fig. 2. Hierarchical clustering heatmap and dendrogram of the tocopherol and FSV content in the seven analyzed industrial hemp accessions.

To evaluate the carotenoid and FSV content in the seven analyzed industrial hemp accessions, a clustering analysis by heatmap was carried out (Fig. 2). The three vitamin forms (δ-tocopherol, menaquinone-7, and δ-tocotrienol) that were not found in all sets of samples were not considered for statistical analysis. The heatmap is correlated to a dendrogram that illustrates the arrangement of the clusters for both the samples and the analytes. The samples belonging to the Carmaleonte variety stood out from the others and were characterized simultaneously by the highest amounts of phytoene, phytofluene, ζ-carotene, and retinol and lowest amounts of β-carotene, 9-*cis*-β-carotene, 15-*cis*-β-carotene, and β-cryptoxanthin. These two clusters of compounds are also visible in the dendrogram of the analytes. Indeed, the combined concentration of phytoene and phytofluene for the Carmaleonte samples (84 μg g^{-1}) was significantly higher than in all other samples (43–65 μg g^{-1}). Conversely, β-carotene was much lower (7.3 μg g^{-1}) than in all other samples (33–53 μg g^{-1}). In the second cluster of samples, two main groups of samples are clustered: one sub-cluster was constituted by the Codimono and Fibranova samples, and the other by the remaining four accessions. Codimono

Table 3
Untargeted HPLC-PDA data used for the tentative identification of carotenoids in industrial hemp inflorescence.

Peak	RT	compound	Calculated λ_{max}[a]	Observed λ (nm)	Reported λ (nm)[c]	Observed% (III/II)	Reported% (III/II)[c]	Observed Q-ratio	Reported Q-ratio
1	9.9	*all-trans*-zeaxanthin	453	425;448;475	428; 450; 478[b]	45	25[b]		
2	10.7	*all-trans*-dihydrolutein	427	409;429;453	408;428;453[b,d]	38	38[b,d]		
3	11.1	*all-trans*-α-cryptoxanthin	448	427;445;474	421;445; 475[b]	55	60[b]		
4	11.6	3–hydroxy-*all-trans*-β-zeacarotene	427	408;430;454	405;428;453[b]	85	n.r.		
5	12.0	*all-trans*-β-cryptoxanthin	453	429;451;478	425;449; 478[b]	25	25[b]		
6	12.3	*all-trans*-zeinoxanthin	448	420;442;471	421;444;472[b]	53	60[b]		
7	12.8	9-*cis*-β-cryptoxanthin	451–447	342;427;449;475	342;427;449;476[e]	25	78[e]	2.1	4.2 [e]
8	13.0	9-*cis*-zeinoxanthin	446–442	337;426;446;477	331;422;446;475[e]	21	7[e]	2.5	9.1 [e]
9	13.2	unknown 1		402;430;455		95			
10	13.5	2-keto-α-carotene	448	423;446;475	423;446;475[b,d]	38	60[b,d]		
11	13.7	2-keto-β-carotene	453	425;450;480	451;476[b,d]	27	n.r.		
12	14.4	*all-trans*-β-carotene-epoxide	445	426;445;478	422;445;472[b]	25	n.r.		
13	14.7	*cis*-β-carotene-epoxide	443–439	345;425;448;476	337,425,449,475[e]	26	17[e]	9.5	2.7[e]
14	16.8	13-*cis*-α-carotene	446–442	343;417;445;479	346,418;446;474[e]	20	18[e]	3.0	2.3[e]
15	17.4	*all-trans*-α-carotene	448	427;447;475	422;445;473[b]	47	55[b]		
16	17.5	13-*cis*-β-carotene	451–447	345;426;454;481	346;427;450;476[f]	14	10[f]	3.0	2.4[f]
17	17.9	unknown 2		424;455;483					
18	18.4	*all-trans*-β-carotene	453	424;453;480	425;450;483[b]	25	25[b]		
19	18.7	*all-trans*-dihydro-β-carotene	427	410;433;461	410;429;454[b]	43	55[b]		
20	19.3	9-*cis*-β-carotene	451–447	345;428;450;485	347;428;452;479[e]	14	14[e]	3.5	4.1[e]
21	19.6	*all-trans*-β-zeacarotene	427	411;430;460	404;428;452[b]	62	n.r.		
22	20.9	9-*cis*-γ-carotene	463–459	348;428;449;477	338;428;450;477[f]	15	30[f]	4.0	5.8[f]
23	21.2	unknown 3		429;450;476		8			
24	21.7	unknown 4		429;450;479		17			
25	22.2	unknown 5		430;452;480		17			

[a] calculated using the Fieser rules (see ref [47]).
[b] see ref [46].
[c] measured in hexane or ethanol unless otherwise stated.
[d] measured in acetone.
[e] see ref [48].
[f] see ref [30].

and Fibranova seemed characterized by the highest concentrations of β-carotene and its cluster of carotenoids. Moreover, they had higher concentrations of phytoene and phytofluene (43–46 and 19–21 μg g^{-1}, respectively) compared to the other sub-cluster (31–40 and 11.6–14 μg g^{-1}, respectively). The sample belonging to the second sub-cluster showed no clear trend in terms of its carotenoid and FSV content, despite the sometimes higher concentration of some minor analytes, e.g., lutein and zeaxanthin in the case of CS, phylloquinone in the case of Carmagnola, and α-tocopherol in Fibrante.

The information gathered by the hierarchical cluster analysis was then confirmed by an unsupervised chemometric approach based on the PCA (Figure S1). Information on the relations among the samples is displayed in the scores plot along the principal components, whereas the interpretation of the compounds can be investigated on the loadings plot. The 19 carotenoids and FSV that were common to all samples were used as variables. The contribution of principal component 1 (PC1) was 36.4%, while PC2 contributed 20.7% of the total variance (when combined, PC1 and PC2 constituted more than 55% of the total variance). The samples are discriminated alongside PC1, with positive values for Carmaleonte, values around zero for Codimono/Fibranova, and negative values for the other accessions. The two subclusters shown in the dendrogram are also partially discriminated alongside PC2, with positive values for Codimono/Fibranova and generally negative values for the other samples. In the loadings plot (Figure S1b), the two clusters of highly-correlated analytes earlier described are also visible.

3.4. Tentative identification of carotenoids in hemp inflorescence by Hplc-PDA

To gain further knowledge on the carotenoid composition of hemp inflorescence, an HPLC-PDA analysis was performed on the hemp pool. Carotenoids were tentatively identified based on their retention behavior and UV–vis spectra with the support of theoretical rules and data in the literature.

The elution patterns of carotenoids have been widely studied [30,45] and can be summarized as follows: (i) the increase of the molecular weight and the conjugation extension corresponds to longer retention (e.g., phytoene < phytofluene); (ii) the presence and number of oxygen groups decrease the retention (e.g., zeaxanthin < β-cryptoxanthin < β-carotene); (iii) the number of cycles decreases the retention (e.g., β-carotene < γ-carotene < lycopene); (iv) β,ε-carotenoids have a lower retention time than β,β-carotenoids (e.g., lutein < zeaxanthin); (v) the location of *cis* double bonds affects the elution order [45] (e.g., 15-*cis*-β-carotene < 13-*cis*-β-carotene < *all-trans*-β-carotene < 9-*cis*-β-carotene).

Because of their extensive double bond conjugation, carotenoids strongly absorb in the UV–vis region of the electromagnetic spectrum exhibiting a characteristic three-peak spectrum [46]. The absorption maximum and the fine structure of the spectra allow the identification of the chromophore. The absorption maximum of the hypothesized structure (wavelength of the central peak, λ_{max}) can theoretically be calculated using the Fieser rules [47], which are valid for polyenes with more than four conjugated double bonds. Furthermore, the degree of the fine structure is commonly expressed as the percentage ratio between the heights of peaks II and III (% III/II). The presence of *cis*-double bonds also affects the UV–vis spectra compared to the *all-trans* isomer: (i) the parameter% III/II decreases; (ii) a hypochromic effect usually occurs; (iii) a hypsochromic effect usually occurs (2–6 nm for mono-*cis* isomers, 10 nm for di-*cis* isomers, and 50 nm for poli-*cis* isomers), (iv) a *cis*-peak (peak B) appears in the UV region. Since the height of peak B increases as the *cis*-double bond is closer to the center of the conjugated system, the ratio between the heights of peaks II and B, measured from the baseline of the spectrum and called Q-ratio, could also be employed for structure evaluation.

In Table 3, the HPLC-PDA results are shown, whereas the UV–vis spectra are shown in Figure S2. Of the 25 extracted peaks, 4 carotenoids were common to the carotenoids analyzed by targeted LC-MS (compounds 1, 5, 18, and 20), 5 carotenoids (compounds 9, 17, 23, 24, and 25) could not be identified, and 16 carotenoids were annotated based on their retention time and UV–vis spectrum. Compounds 2–4, 6, 15, 19, and 21 were annotated as *all-trans* carotenoid compounds following the match with the predicted λ_{max} and the experimental spectrum and reported fine structure in the Carotenoids Handbook by Britton et al. [46]. For example, compound 15 was tentatively identified as *all-trans*-α-carotene. The experimental λ_{max} (447 nm) was in very good agreement with the one calculated by the Fieser rules (448 nm); moreover, the experimental fine structure (427;447;475 nm) and% III/II (47) were in agreement with the reported values (422;445;473 nm and 55, respectively); finally, according to the retention time behavior rules of carotenoids, *all-trans*-α-carotene eluted earlier (17.4 min) than the β isomer (18.4 min). Three other carotenoids (compounds 12–14) were similarly identified as keto- and epoxy-derivatives of α-carotene and β-carotene. It is worth mentioning that for these compounds either the reported fine structures were measured in acetone or the parameter% III/II was not available. Finally, six *cis*-carotenoids were identified based on the variations of their retention times and UV–vis spectra compared to the *all-trans* isomers and confirmed by data in the literature [30,48]. For example, compound 14 was tentatively identified as 13-*cis*-α-carotene since it eluted earlier (16.8 min) than the *all-trans* isomer (17.4 min) and showed a hypsochromic effect on λ_{max} (445 vs 447 nm of the *all-trans* isomer), a reduced% III/II (20 vs 47 of the *all-trans* isomer), and the appearance of a *cis*-peak at 343 nm. The parameters were also in good agreement with previously reported data in the literature [48]. All other *cis*-carotenoids were identified with the same rationale.

4. Conclusions

Cannabis sativa has long captured the attention of researchers for its high content of biologically active compounds. Although most studies on *Cannabis* are addressed to cannabinoids, it has been proven that minor constituents significantly contribute to the healthy effect of *Cannabis* extracts. For the first time, the carotenoid and FSV profile of *Cannabis* inflorescences has extensively been characterized in both qualitative and quantitative fashion after an extraction approach aimed at avoiding the generation of artifacts. The analysis of seven industrial hemp varieties grown in the same site and pedoclimatic conditions showed once again that the genomic variability of *Cannabis* varieties significantly affects the expression of phytocompounds. Further investigation, involving samples grown in different geographic areas, the season, and the flowering stage, is needed to extend the knowledge on micronutrients in *Cannabis* inflorescence.

Declaration of Competing Interest

The authors declare that they have no known competing financial interests or personal relationships that could have appeared to influence the work reported in this paper.

CRediT authorship contribution statement

Andrea Cerrato: Writing – original draft, Formal analysis, Visualization. **Sara Elsa Aita:** Investigation, Funding acquisition. **Giuseppe Cannazza:** Supervision, Funding acquisition. **Anna Laura Capriotti:** Conceptualization, Writing – review & editing, Supervision. **Chiara Cavaliere:** Writing – review & editing. **Cinzia Citti:** Investigation. **Chiara Dal Bosco:** Methodology. **Alessandra Gentili:** Methodology. **Carmela Maria Montone:** Investigation, Validation. **Roberta Paris:** Resources, Funding acquisition. **Aldo Laganà:** Conceptualization, Project administration.

Data availability

Data will be made available on request.

Acknowledgements

The authors would like to thank Dr. Ilaria Alberti and Dr. Massimo Montanari for their effort in managing the experimental field in “Busa Carrare” farm located in Rovigo. The plant material was supplied within the UNIHEMP research project “Use of iNdustrIal Hemp biomass for Energy and new biocheMicals Production” (ARS01_00668) funded by European Regional Development Fund (within the PON R&I 2017–2020– Axis 2 – Action II – OS 1.b). Grant decree UNIHEMP prot. no. 2016 of 27/07/2018; CUP B76C18000520005

This work was also supported by Avvio alla Ricerca 2021 project “Large-scale profiling of carotenoids in Cannabis sativa L. inflorescences from different dioecious cultivars grown in Italy by liquid chromatography photodiode array detection and triple quadrupole linear ion trap mass spectrometry” funded by Sapienza University of Rome, protocol number: AR12218167657CE4.

Supplementary materials

Supplementary material associated with this article can be found, in the online version, at doi:10.1016/j.chroma.2023.463838.

References

[1] T. Hussain, G. Jeena, T. Pitakbut, N. Vasilev, O. Kayser, Cannabis sativa research trends, challenges, and new-age perspectives, IScience 24 (2021) 103391, doi:10.1016/j.isci.2021.103391.
[2] E. Small, Evolution and classification of cannabis sativa (Marijuana, Hemp) in relation to human utilization, Bot. Rev. 81 (2015) 189–294, doi:10.1007/s12229-015-9157-3.
[3] E.M. Wimalasiri, E. Jahanshiri, V.G.P. Chimonyo, N. Kuruppuarachchi, T.A.S.T.M. Suhairi, S.N. Azam-Ali, P.J. Gregory, A framework for the development of hemp (Cannabis sativa L.) as a crop for the future in tropical environments, Ind. Crops. Prod. 172 (2021) 113999, doi:10.1016/j.indcrop.2021.113999.
[4] C.M. Andre, J.-F. Hausman, G. Guerriero, Cannabis sativa: the plant of the thousand and one molecules, Front. Plant Sci. 7 (2016), doi:10.3389/fpls.2016.00019.
[5] F. Pellati, V. Borgonetti, V. Brighenti, M. Biagi, S. Benvenuti, L. Corsi, Cannabis sativa L. and nonpsychoactive cannabinoids: their chemistry and role against oxidative stress, inflammation, and cancer, Biomed. Res. Int. 2018 (2018) 1–15, doi:10.1155/2018/1691428.
[6] C.M. Montone, A. Cerrato, B. Botta, G. Cannazza, A.L. Capriotti, C. Cavaliere, C. Citti, F. Ghirga, S. Piovesana, A. Laganà, Improved identification of phytocannabinoids using a dedicated structure-based workflow, Talanta 219 (2020) 121310, doi:10.1016/j.talanta.2020.121310.
[7] E. Mazzara, J. Torresi, G. Fico, A. Papini, N. Kulbaka, S. Dall'Acqua, S. Sut, S. Garzoli, A.M. Mustafa, L. Cappellacci, D. Fiorini, F. Maggi, C. Giuliani, R. Petrelli, A comprehensive phytochemical analysis of terpenes, polyphenols and cannabinoids, and micromorphological characterization of 9 commercial varieties of cannabis sativa L., Plants. 11 (2022) 891. https://doi.org/10.3390/plants11070891.
[8] G. Micalizzi, F. Alibrando, F. Vento, E. Trovato, M. Zoccali, P. Guarnaccia, P. Dugo, L. Mondello, Development of a novel microwave distillation technique for the isolation of cannabis sativa l. essential oil and gas chromatography analyses for the comprehensive characterization of terpenes and terpenoids, including their enantio-distribution, Molecules 26 (2021) 1588, doi:10.3390/molecules26061588.
[9] G. Micalizzi, F. Vento, F. Alibrando, D. Donnarumma, P. Dugo, L. Mondello, Cannabis Sativa L.: a comprehensive review on the analytical methodologies for cannabinoids and terpenes characterization, J. Chromatogr. A. 1637 (2021) 461864, doi:10.1016/j.chroma.2020.461864.
[10] A. Cerrato, G. Cannazza, A.L. Capriotti, C. Citti, G. La Barbera, A. Laganà, C.M. Montone, S. Piovesana, C. Cavaliere, A new software-assisted analytical workflow based on high-resolution mass spectrometry for the systematic study of phenolic compounds in complex matrices, Talanta 209 (2020) 120573, doi:10.1016/j.talanta.2019.120573.
[11] M. Antonelli, B. Benedetti, G. Cannazza, A. Cerrato, C. Citti, C.M. Montone, S. Piovesana, A. Laganà, M. Antonelli, B. Benedetti, G. Cannazza, A. Cerrato, C. Citti,

C.M. Montone, S. Piovesana, A. Laganà, New insights in hemp chemical composition: a comprehensive polar lipidome characterization by combining solid phase enrichment, high-resolution mass spectrometry, and cheminformatics, Anal. Bioanal. Chem. 412 (2020) 413–423, doi:10.1007/s00216-019-02247-6.
[12] S. Piovesana, S.E. Aita, G. Cannazza, A.L. Capriotti, C. Cavaliere, A. Cerrato, P. Guarnaccia, C.M. Montone, A. Laganà, In-depth cannabis fatty acid profiling by ultra-high performance liquid chromatography coupled to high resolution mass spectrometry, Talanta 228 (2021) 122249, doi:10.1016/j.talanta.2021.122249.
[13] P. Arena, F. Rigano, P. Guarnaccia, P. Dugo, L. Mondello, E. Trovato, Elucidation of the lipid composition of hemp (Cannabis sativa L.) products by means of gas chromatography and ultra-high performance liquid chromatography coupled to mass spectrometry detection, Molecules 27 (2022) 3358, doi:10.3390/molecules27103358.
[14] M.M. Radwan, S. Chandra, S. Gul, M.A. ElSohly, Cannabinoids, phenolics, terpenes and alkaloids of cannabis, Molecules 26 (2021) 2774, doi:10.3390/molecules26092774.
[15] J.L. Bautista, S. Yu, L. Tian, Flavonoids in cannabis sativa : biosynthesis, bioactivities, and biotechnology, ACS Omega 6 (2021) 5119–5123, doi:10.1021/acsomega.1c00318.
[16] A.J. Meléndez-Martínez, A.I. Mandić, F. Bantis, V. Böhm, G.I.A. Borge, M. Brnčić, A. Bysted, M.P. Cano, M.G. Dias, A. Elgersma, M. Fikselová, J. García-Alonso, D. Giuffrida, V.S.S. Gonçalves, D. Hornero-Méndez, K. Kljak, V. Lavelli, G.A. Manganaris, P. Mapelli-Brahm, M. Marounek, B. Olmedilla-Alonso, M.J. Periago-Castón, A. Pintea, J.J. Sheehan, V. Tumbas Šaponjac, M. Valšíková-Frey, L. Van Meulebroek, N. O'Brien, A comprehensive review on carotenoids in foods and feeds: status quo, applications, patents, and research needs, Crit. Rev. Food Sci. Nutr. 62 (2022) 1999–2049, doi:10.1080/10408398.2020.1867959.
[17] C.E. Ofoedu, J.O. Iwouno, E.O. Ofoedu, C.C. Ogueke, V.S. Igwe, I.M. Agunwah, A.F. Ofoedum, J.S. Chacha, O.P. Muobike, A.O. Agunbiade, N.E. Njoku, A.A. Nwakaudu, N.E. Odimegwu, O.E. Ndukauba, C.U. Ogbonna, J. Naibaho, M. Korus, C.O.R. Okpala, Revisiting food-sourced vitamins for consumer diet and health needs: a perspective review, from vitamin classification, metabolic functions, absorption, utilization, to balancing nutritional requirements, PeerJ 9 (2021) e11940, doi:10.7717/peerj.11940.
[18] S.A. Tanumihardjo, R.M. Russell, C.B. Stephensen, B.M. Gannon, N.E. Craft, M.J. Haskell, G. Lietz, K. Schulze, D.J. Raiten, Biomarkers of nutrition for development (BOND)—vitamin a review, J. Nutr. 146 (2016) 1816S–1848S, doi:10.3945/jn.115.229708.
[19] S. Shah, Y. Shiekh, J.A. Lawrence, F. Ezekwueme, M. Alam, S. Kunwar, D.K. Gordon, A systematic review of effects of Vitamin E on the cardiovascular system, Cureus (2021), doi:10.7759/cureus.15616.
[20] J.J. DiNicolantonio, J. Bhutani, J.H. O'Keefe, The health benefits of vitamin K, Open Hear. 2 (2015) e000300, doi:10.1136/openhrt-2015-000300.
[21] T. Maoka, Carotenoids as natural functional pigments, J. Nat. Med. 74 (2020) 1–16, doi:10.1007/s11418-019-01364-x.
[22] S.A.E. Heider, P. Peters-Wendisch, R. Netzer, M. Stafnes, T. Brautaset, V.F. Wendisch, Production and glucosylation of C50 and C40 carotenoids by metabolically engineered Corynebacterium glutamicum, Appl. Microbiol. Biotechnol. 98 (2014) 1223–1235, doi:10.1007/s00253-013-5359-y.
[23] M. Spano, G. Di Matteo, C. Ingallina, B. Botta, D. Quaglio, F. Ghirga, S. Balducci, S. Cammarone, E. Campiglia, A.M. Giusti, G. Vinci, M. Rapa, S. Ciano, L. Mannina, A.P. Sobolev, A multimethodological characterization of cannabis sativa L. Inflorescences from seven dioecious cultivars grown in Italy: the effect of different harvesting stages, Molecules 26 (2021) 2912, doi:10.3390/molecules26102912.
[24] M. Irakli, E. Tsaliki, A. Kalivas, F. Kleisiaris, E. Sarrou, C.M. Cook, Effect of genotype and growing year on the nutritional, phytochemical, and antioxidant properties of industrial hemp (Cannabis sativa L.) seeds, Antioxidants 8 (2019) 491, doi:10.3390/antiox8100491.
[25] A. Aiello, F. Pizzolongo, G. Scognamiglio, A. Romano, P. Masi, R. Romano, Effects of supercritical and liquid carbon dioxide extraction on hemp (Cannabis sativa L.) seed oil, Int. J. Food Sci. Technol. 55 (2020) 2472–2480, doi:10.1111/ijfs.14498.
[26] J. Liang, A. Appukuttan Aachary, U. Thiyam-Holländer, Hemp seed oil: minor components and oil quality, Lipid Technol. 27 (2015) 231–233, doi:10.1002/lite.201500050.
[27] A. Cerrato, C. Citti, G. Cannazza, A.L. Capriotti, C. Cavaliere, G. Grassi, F. Marini, C.M. Montone, R. Paris, S. Piovesana, A. Laganà, Phytocannabinomics: untargeted metabolomics as a tool for cannabis chemovar differentiation, Talanta 230 (2021) 122313, doi:10.1016/j.talanta.2021.122313.
[28] S. Mishchenko, J. Mokher, I. Laiko, N. Burbulis, H. Kyrychenko, S. Dudukova, Phenological growth stages of hemp (Cannabis sativa L.): codification and description according to the BBCH scale, Žemės Ūkio Moksl 24 (2017), doi:10.6001/zemesukiomokslai.v24i2.3496.
[29] C. Nimalaratne, C. Sun, J. Wu, J.M. Curtis, A. Schieber, Quantification of selected fat soluble vitamins and carotenoids in infant formula and dietary supplements using fast liquid chromatography coupled with tandem mass spectrometry, Food Res. Int. 66 (2014) 69–77, doi:10.1016/j.foodres.2014.08.034.
[30] A. Gentili, F. Caretti, S. Ventura, V. Pérez-Fernández, A. Venditti, R. Curini, Screening of carotenoids in tomato fruits by using liquid chromatography with diode array–linear ion trap mass spectrometry detection, J. Agric. Food Chem. 63 (2015) 7428–7439, doi:10.1021/acs.jafc.5b02910.
[31] K. Nagy, M.-.C. Courtet-Compondu, B. Holst, M. Kussmann, Comprehensive analysis of Vitamin E constituents in human plasma by liquid chromatography−mass spectrometry, Anal. Chem. 79 (2007) 7087–7096, doi:10.1021/ac0708689.
[32] Commission Decision (2002/657 /EC) of 12 August 2002 implementing Council Directive 96/23 / EC concerning the performance of analytical methods and the interpretation of results. Off. J. Eur. Comm. L 221, Brussels, Belgium, p. 8., (n.d.).
[33] K. Hasegawa, K. Minakata, M. Suzuki, O. Suzuki, The standard addition method and its validation in forensic toxicology, Forensic Toxicol 39 (2021) 311–333, doi:10.1007/s11419-021-00585-8.
[34] J. Xia, D.S. Wishart, Metabolomic DATA processing, analysis, and interpretation using metaboanalyst, Curr. Protoc. Bioinforma. (2011) 34, doi:10.1002/0471250953.bi1410s34.
[35] R.K. Saini, Y.-.S. Keum, Carotenoid extraction methods: a review of recent developments, Food Chem 240 (2018) 90–103, doi:10.1016/j.foodchem.2017.07.099.
[36] A.Z. Mercadante, D.B. Rodrigues, F.C. Petry, L.R.B. Mariutti, Carotenoid esters in foods - a review and practical directions on analysis and occurrence, Food Res. Int. 99 (2017) 830–850, doi:10.1016/j.foodres.2016.12.018.
[37] A. Gentili, F. Caretti, S. Bellante, S. Ventura, S. Canepari, R. Curini, Comprehensive profiling of carotenoids and fat-soluble vitamins in milk from different animal species by LC-DAD-MS/MS hyphenation, J. Agric. Food Chem. 61 (2013) 1628–1639, doi:10.1021/jf302811a.
[38] T. Li, J. Xu, H. Wu, G. Wang, S. Dai, J. Fan, H. He, W. Xiang, A saponification method for chlorophyll removal from microalgae biomass as oil feedstock, Mar. Drugs. 14 (2016) 162, doi:10.3390/md14090162.
[39] A.T. Soares, D.C. da Costa, A.A.H. Vieira, N.R. Antoniosi Filho, Analysis of major carotenoids and fatty acid composition of freshwater microalgae, Heliyon 5 (2019) e01529, doi:10.1016/j.heliyon.2019.e01529.
[40] B. Hrvolová, M. Martínez-Huélamo, M. Colmán-Martínez, S. Hurtado-Barroso, R. Lamuela-Raventós, J. Kalina, Development of an Advanced HPLC–MS/MS method for the determination of carotenoids and fat-soluble vitamins in human plasma, Int. J. Mol. Sci. 17 (2016) 1719, doi:10.3390/ijms17101719.
[41] M. Shumskaya, E.T. Wurtzel, The carotenoid biosynthetic pathway: thinking in all dimensions, Plant Sci. 208 (2013) 58–63, doi:10.1016/j.plantsci.2013.03.012.
[42] N.J. Engelmann, S.K. Clinton, J.W. Erdman, Nutritional aspects of phytoene and phytofluene, carotenoid precursors to Lycopene, Adv. Nutr. 2 (2011) 51–61, doi:10.3945/an.110.000075.
[43] A. During, A. Nagao, J. Terao, β-Carotene 15,15′-Dioxygenase activity and cellular retinol-binding protein Type II level are enhanced by dietary unsaturated triacylglycerols in rat intestines, J. Nutr. 128 (1998) 1614–1619, doi:10.1093/jn/128.10.1614.
[44] S. Montserrat-de la Paz, F. Marín-Aguilar, M.D. García-Giménez, M.A. Fernández-Arche, Hemp (Cannabis sativa L.) seed oil: analytical and phytochemical characterization of the unsaponifiable fraction, J. Agric. Food Chem. 62 (2014) 1105–1110, doi:10.1021/jf404278q.
[45] A.J. Meléndez-Martínez, M.L. Escudero-Gilete, I.M. Vicario, F.J. Heredia, Separation of structural, geometrical and optical isomers of epoxycarotenoids using triacontyl-bonded stationary phases, J. Sep. Sci. 32 (2009) 1838–1848, doi:10.1002/jssc.200800717.
[46] G. Britton, S. Liaaen-Jensen, H. Pfander, Carotenoids handbook, Birkhauser Verlag Basel, Switzerland, 2008 (n.d.).
[47] L.F. FIESER, Absorption spectra of carotenoids; structure of vitamin A 2, J. Org. Chem. 15 (1950) 930–943, doi:10.1021/jo01151a003.
[48] A. Gentili, C. Dal Bosco, S. Fanali, C. Fanali, Large-scale profiling of carotenoids by using non aqueous reversed phase liquid chromatography – photodiode array detection – triple quadrupole linear ion trap mass spectrometry: application to some varieties of sweet pepper (Capsicum annuum L.), J. Pharm. Biomed. Anal. 164 (2019) 759–767, doi:10.1016/j.jpba.2018.11.042.